Study of thermal effects on stress wave propagation in polymeric material of plate-like shape

R. Hayasi（林　良英）

Abstract

Stress wave propagation in viscoelastic materials has been a problem of interest in geophysics, fracture mechanics and nondestructive engineering for many years. Propagation behavior of stress waves in plates is generally affected by the wavelength and the dimensions and temperature of the plates. The thermal effects on stress wave propagation in axially impacted polymeric material of plate-like shape have been investigated for the case in which the ratio of wavelength to lateral dimensions is constant. Strain gage with the aid of dynamic photoelastic technique was utilized to examine the influence of temperature on propagation speed and attenuation coefficient of stress waves in rectangular epoxy resin bar. The results show that the stress wave speed as a function of temperature is in reasonable agreement with theoretical predictions for longitudinal waves as derived from a modified Love's equation involving the thermal effects.

Keywords: Stress waves; Polymeric material; Thermal effects; Plates

1. Introduction

Stress wave propagation in viscoelastic materials for laboratory experiments and simulations has been a wide variety of problems

in fields such as geophysics, fracture mechanics, nondestructive engineering and mining engineering for many years. Propagation behavior of stress waves in a bounded homogeneous solid is generally influenced by the wavelength and the geometrical shape and temperature of the medium. Propagation speed and attenuation of stress waves in a viscoelastic bar of plate-like shape at a constant temperature depend on the ratio of wavelength to lateral dimensions when the wavelength is comparable with the lateral dimensions of the bar (Hayasi et al., 2008). The temperature dependence of mechanical and acoustic properties for many polymers and other viscoelastic materials has been studied over a wide range of temperature. Kawata (1956) and Tuzi et al. (1958) examined the variation of the mechanical and photoelastic properties, or elastic modulus and stress-optical coefficient, with temperature for various cross-linked polymers under constant tension stresses. Nguyen et al. (1995) measured the temperature dependence of acoustic and mechanical properties of homogeneous and heterogeneous polymers by ultrasonic and dynamic mechanical methods and studied both glass transition and the sub-glass relaxation at different frequencies. Nomura et al. (2003) examined the sound velocity in the high-strength fiber-reinforced plastics over a wide temperature range by the sound pulse transmission method.

A semiconductor strain gage is a device for detecting the dynamic strain of a solid, and it gives data at a discrete location on the sample surface continuously in time. The wave patterns such as longitudinal, flexural, and torsional waves produced due to impact force can not be clearly detected by the strain gage. On the other hand, dynamic photoelasticity, a technique based on the concept of transparent material birefringence, is an experimental method for stress analysis of dynamic problems such as stress wave propagation and dynamic stress concentration, and it provides information continuously in the full stress wave field inside a sample at discrete times over an entire dynamic event. In impact tests the wave patterns can be directly observed by the use of the high-speed photoelastic technique. Hence, the strain gage

measurements in combination with the dynamic photoelasticity make stress wave analysis more reliable.

In this work, we carried out experiments on propagation behavior of stress waves in axially impacted epoxy resin bar of rectangular cross-section at different temperatures below the glass transition temperature by a semiconductor strain gage with the aid of dynamic photoelasticity and studied the thermal effects on the propagation speed and attenuation coefficient of stress waves for the case in which the ratio of half-wavelength to larger lateral dimension is about 2. Thermosetting epoxy resin used for the propagation medium of stress waves is an amorphous polymer bonded in a three dimensional network with a high degree of crosslinking and exhibits stress-induced birefringence.

2. Experimental

The experimental arrangement consists basically of a semiconductor strain gage, dynamic photoelastic apparatus associated with the Cranz-Schardin high-speed camera, air gun, thermal container, and digital oscilloscope (Hayasi et al., 2008). The polariscope used in photoelasticity is composed of an analyzer, polarizer, light source, field lens, and two quarter-wave plates. A light beam from each of nine spark gaps in dynamic photoelastic apparatus is focused on an individual camera lens to establish nine images on a sheet of film (FUJIFILM NEOPAN 100 black and white film). A xenon flash lamp with a single wavelength 546 nm was used as the light source. The main advantage of the dynamic photoelastic method is that the stress wave field is visualized inside a solid and in exciting a bounded solid the longitudinal, flexural, and torsional waves can be observed. A thermal container and air gun shown in Fig. 1 (a) are placed in the center with a dynamic photoelastic system which is based on the optical one of two-dimensional photoelasticity. The thermal container for measurement in higher temperature region consists of a heat-insulating box and the Nichrome

wire and is designed to open and close both movable side faces in order to transmit a beam of light through the specimen placed in it. Figure 1 (b) shows the schematic drawing of thermal container for lower temperature region. The vapor of liquid nitrogen was used as the cooling medium. A 6-mm-caliber air gun and an air pressure of 30 kPa were used to generate a compressive stress pulse in the rectangular epoxy bar, and the projectile was a cylindrical steel of diameter 5.8 mm, length 12.5 mm, and mass 2.5 g. Two aluminum foils were pasted on the impacted end face of a specimen and the air gun barrel, respectively, and were connected to the delay circuit unit and digital oscilloscope through the trigger circuit unit shown in Fig. 1 (c). When a projectile fired from the air gun hits on the end face of specimen, the collision of the projectile with the specimen causes an electrical connection between two contact points, and this electrical connection is used as the trigger for strain gage measurement and dynamic photoelastic recording. The projectile was fired after keeping the specimen in the thermal container for about 30 minutes at each temperature, and the end of the specimen opposite the impacted end was free. If a projectile impinges on the end face of specimen, then the strain-time relationship is detected using a semiconductor strain gage (Kyowa 1 mm gage length, Type KSP-1-350-E4) mounted on the center of the top surface of the specimen, and simultaneously the photoelastic fringe patterns in real time are observed by the high-speed photoelastic method. The output of the strain gage is fed to a digital oscilloscope (Iwatsu, Type DS-8812) through a bridge circuit unit, and then the oscilloscope trace is transferred to a computer for processing. The time intervals between the spark gaps producing the separate images for dynamic photoelastic recording are measured with a photosensor (Hamamatsu, Type C4890) and digital oscilloscope and are accurate to 1 μs.

The sample studied was rectangular epoxy bar of width 12 mm, thickness 6 mm, and length 201 mm, and the thermosetting epoxy resin prepared from Araldite CT200 and epoxy solvent HT901 in the weight percentage of 78 to 22 was purchased from the Rikoken.

3. Results

Figures 2 and 3 show the typical results for the dynamic isochromatic fringe patterns recorded with high-speed photoelastic system and the fringe order distributions identified by isochromatic fringe patterns in epoxy resin bar of rectangular cross-section at 21℃ and 60℃, respectively. These results show the generation and the subsequent evolution of stress wave propagation events that occur on a microsecond time-scale after projectile impact. In the photographs of isochromatic fringe pattern, the stress pulse of compression generated after projectile impact travels from the impacted end towards the free end and reflects from the nonimpacted end as a pulse of tension. This pulse of tension travels back and reflects from the impacted end as a pulse of compression. The whole cycle is then repeated. It may be seen that the stress wave pulse becomes small near the free end because of the superposition of the incident and reflected waves. Thus the fringe order distribution corresponding to the stress wave pulse propagates through the specimen, and the location of the stress wave pulse can be estimated as a function of time. From the dynamic isochromatic fringe patterns for a rectangular epoxy bar in Figs. 2 and 3, the propagation speeds of the fringes at 21℃ and 60℃ are estimated as 1.69 km/s and 1.62 km/s, respectively.

Figure 4 shows the typical examples of the strain–time relationship detected by a semiconductor strain gage mounted on the center of the top surface of the bar. In these strain–time curves, the negative strain corresponds to a stress pulse of compression, and the positive strain corresponds to a stress pulse of tension. The time between successive maximum peaks, or successive minimum peaks, in the curves gives the time in which the stress wave travels back and forth once along the bar. Hence the speed of propagation of stress waves can be estimated by measuring the intervals between successive reflected pulses in the strain–time curve. If t_1 is the time at which the first minimum, or maximum, peak is produced and t_n is the time at which the n-th

minimum, or maximum, peak is produced, the propagation speed c_l of longitudinal stress waves is given as

$$c_l = \frac{2(n-1)L}{t_n - t_1}, \tag{1}$$

where L is the length of the specimen. From the strain–time relations in Fig. 4, with help of Eq. (1), the speeds of longitudinal stress wave propagated along the sample at 21℃ and 60℃ are estimated as 1.691 km/s and 1.624 km/s, respectively. These longitudinal wave speeds obtained from the strain gage output coincide well with the values, 1.69 km/s at 21℃ and 1.62 km/s at 60℃, measured from the speed of fringes, respectively. The wavelength λ of the impact stress pulse must be determined as the product of the duration of the first stress pulse and the propagation speed of the stress pulse in the strain–time curve because the superposition of the transmitted wave and the wave reflected at the side face of the bar broadens the duration of the stress wave pulse as the pulse travels along the specimen. From the experimental curves in Fig. 4, the wavelengths of a stress wave at 21℃ and 60℃ are estimated as 4.99×10^{-2}m and 4.98×10^{-2}m, respectively. The spatial attenuation coefficient α for the amplitude of a stress wave can be calculated using a least-squares method from the strain–time relation and is estimated to be 0.397m^{-1} at 21℃ and 0.231m^{-1} at 60℃.

From our experimental data on the dynamic strain in the temperature range from –61℃ to 60℃, the longitudinal stress wave speed plotted against temperature for rectangular epoxy bar of width 12 mm, thickness 6 mm, and length 201 mm is presented in Fig. 5. Figure 6 shows the variation of attenuation coefficient with temperature.

4. Discussion

The thermal effects on stress wave propagation in the epoxy resin bar of rectangular cross-section are investigated theoretically by means of a modified Love's wave equation and thermodynamic method.

In terms of the temperature T, volume V, pressure P, and entropy S, the thermodynamic relation may be written

$$\left(\frac{\partial V}{\partial P}\right)_S = \left(\frac{\partial V}{\partial P}\right)_T + \frac{T}{C_P V}\left(\frac{\partial V}{\partial T}\right)_P^2 , \tag{2}$$

where C_P is the heat capacity per unit volume at constant pressure (Landau and Lifshitz, 1986). The ordinary isothermal bulk modulus k and the adiabatic bulk modulus $k(T)$ are, respectively, given by

$$\frac{1}{k} = \frac{1}{V}\left(\frac{\partial V}{\partial P}\right)_T , \qquad \frac{1}{k(T)} = \frac{1}{V}\left(\frac{\partial V}{\partial P}\right)_S ,$$

so that from Eq. (2) the relation between k and $k(T)$ for the material can be represented by

$$\frac{1}{k(T)} = \frac{1}{k} + \frac{\beta^2}{C_P} T \tag{3}$$

where $\beta = V^{-1}(\partial V/\partial T)_\rho$ is the coefficient of volume thermal expansion. Young's modulus for an elastic material is given by $9\mu k/(3k+\mu)$, μ being the shear modulus (Kolsky, 1963), so that from Eq. (3) the temperature-dependent Young's modulus can be approximately written as $E_0(1-bT)$ for a perfectly elastic medium, where E_0 is Young's modulus at absolute zero and $b = \beta^2 E_0/9C_P$ is sufficiently small compared to unity. On the other hand, an empirical expression for T-dependent Young's modulus proposed by Wachtman et al. (1961) is given by $E(T) = E_0 - BT\exp(-T_C/T)$, where the phenomenological constant T_C is connected to the Debye temperature and B is related to the coefficient of volume thermal expansion and the specific heat (Anderson, 1966). Hence, thermal depression of the Young's modulus for an imperfectly elastic material may be assumed to be expressed as

$$\frac{E(T)}{E_0} = 1 - \alpha T \exp\left(-\frac{T_C}{T}\right) . \tag{4}$$

From the experimental data on the temperature dependence of Young's modulus of epoxy resin measured by Kawata (1956) and Tuzi et al. (1958), we have $E_0 = 5000\text{MPa}$, $\alpha = 2.55\times10^{-3}\text{K}^{-1}$, and $T_C = 180\text{K}$ in Eq. (4). The density of the medium at temperature T is approximately given by

$$\rho(T) = \rho_0(1 - \beta T), \tag{5}$$

where ρ_0 is the density at absolute zero. The material constants of the epoxy resin tested are $\rho(288) = 1205\text{kg/m}^3$, $\beta = 2.78 \times 10^{-4}\text{K}^{-1}$ and Poisson's ratio $\nu = 0.407$.

The wave equation involving the geometric effects due to lateral inertia for the longitudinal displacement u of stress waves in the x direction normal to the cross-section in the bar of plate-like shape takes the form

$$\frac{\partial^2 u}{\partial t^2} - \nu^2 K^2 \frac{\partial^4 u}{\partial x^2 \partial t^2} = \frac{E}{\rho(1-\nu^2)} \frac{\partial^2 u}{\partial x^2}, \tag{6}$$

where K is the radius of gyration of a cross-section about the neutral axis of the bar (Love, 1944 and Hayasi et al., 2008). By the use of the modified Love's wave equation (6) involving the thermal effects with Eqs. (4) and (5), the propagation speed $c_l(T)$ of longitudinal stress waves in a bar of rectangular cross-section at T is given by

$$c_l(T) = \sqrt{\frac{E_0[1 - \alpha T \exp(-T_C/T)]}{\rho_0(1-\beta T)(1-\nu^2)(1 + 4\pi^2 K^2 \nu^2/\lambda^2)}}. \tag{7}$$

For a rectangular bar K is equal to $(w^2+h^2)/12$, where w and h are the sides of the rectangular sections.

Figure 5 shows a comparison between the experimental values on plotting the stress wave speed against temperature and the theoretical curve obtained from Eq. (7) for rectangular epoxy bar of width 12 mm, thickness 6 mm, and length 201 mm. It may be seen that reasonable agreement has been obtained. The variation of attenuation coefficient of the stress wave with temperature is shown in Fig. 6. It may be seen from this figure that the damping falls off rapidly near 0℃ with increasing temperature.

5. Conclusions

Experimental studies have been conducted using a semiconductor

strain gage and dynamic photoelasticity to investigate the thermal effects on stress wave propagation in rectangular epoxy resin bar of width 12 mm, thickness 6 mm, and length 201 mm for the case in which the half-wavelength is about two times the larger side of cross-section. The propagation speed and attenuation coefficient of longitudinal stress waves in the temperature range from –61℃ to 60℃ were evaluated from the dynamic strain detected by the semiconductor strain gage with the aid of high-speed photoelasticity. It was found that the variation of longitudinal stress wave speed with temperature is in reasonable agreement with the theoretical curve predicted by a modified Love's equation involving the thermal effects. The attenuation coefficient of the longitudinal wave decreases with temperature and falls off rapidly near 0℃.

References

Anderson, O.L., 1966. Derivation of Wachtman's Equation for the Temperature Dependence of Elastic Moduli of Oxide Compounds. Phys. Rev. 144, 553-557.

Hayasi, R., Masuda, Y., Hashimoto, S., Kuriyama, S., 2008. Analysis of geometric effects on stress wave propagation in epoxy resins of plate-like structure by dynamic photoelasticity combined with strain gauge. Jpn. J. Appl. Phys. 47, 4676-4681.

Kawata, K., 1956. Variation of photoelastic behavior with temperature for some polymers. J. Polym. Sci. 19, 359-364.

Kolsky, H., 1963. Stress waves in Solids. Dover Publications, New York, pp. 9-10.

Landau, L.D., Lifshitz, E.M., 1986. Theory of Elasticity: 3rd Edition. Pergamon, Oxford, UK, p. 15.

A. E. H. Love, A.E.H., 1944. A Treatise on the Mathematical Theory of Elasticity: 4th Edition. Dover Publications, New York, p. 428.

Nguyen, N.T., Lethiecq, M., Gerard, J.F., 1995. Glass transition characterization of homogeneous and heterogeneous polymers by an

ultrasonic method. Ultrasonics 33, 323-329.
Nomura, R., Yoneyama, K., Ogasawara, F., Ueno, M., Okuda, Y., Yamanaka, A., 2003. Temperature dependence of sound velocity in high-strength fiber-reinforced plastics. Jpn. J. Appl. Phys. 42, 5205-5207.
Tuzi, Z., Kawata, K., Hori, I., 1958. The photoelastic behaviour of cross-linked polymers. Br. J. Appl. Phys. 9, 173-178.
Wachtman, J.B., Tefft, W.E., Lam, D.G.. Apstein, C.S., 1961. Exponential Temperature Dependence of Young's Modulus for Several Oxides. Phys. Rev. 122, 1754-1759.

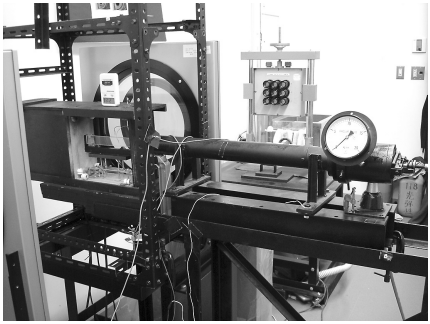

(a)

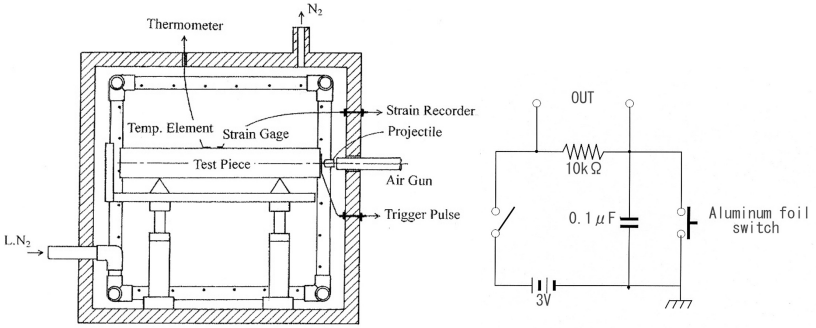

(b) (c)

Fig. 1. A thermal container for high temperature measurement and an air gun (a), schematic drawings of thermal container for measurement at lower temperatures (b), and trigger circuit unit (c).

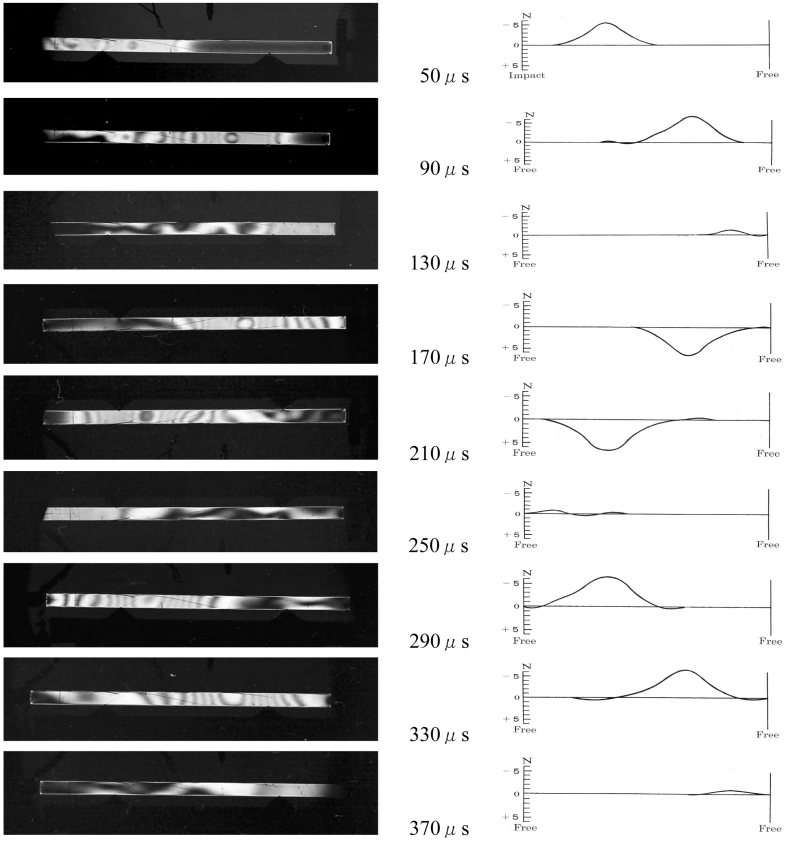

Fig. 2. Dynamic isochromatic fringe patterns and fringe order distributions in rectangular epoxy bar at 21℃. Times given are measured from the instant of direct projectile impact.

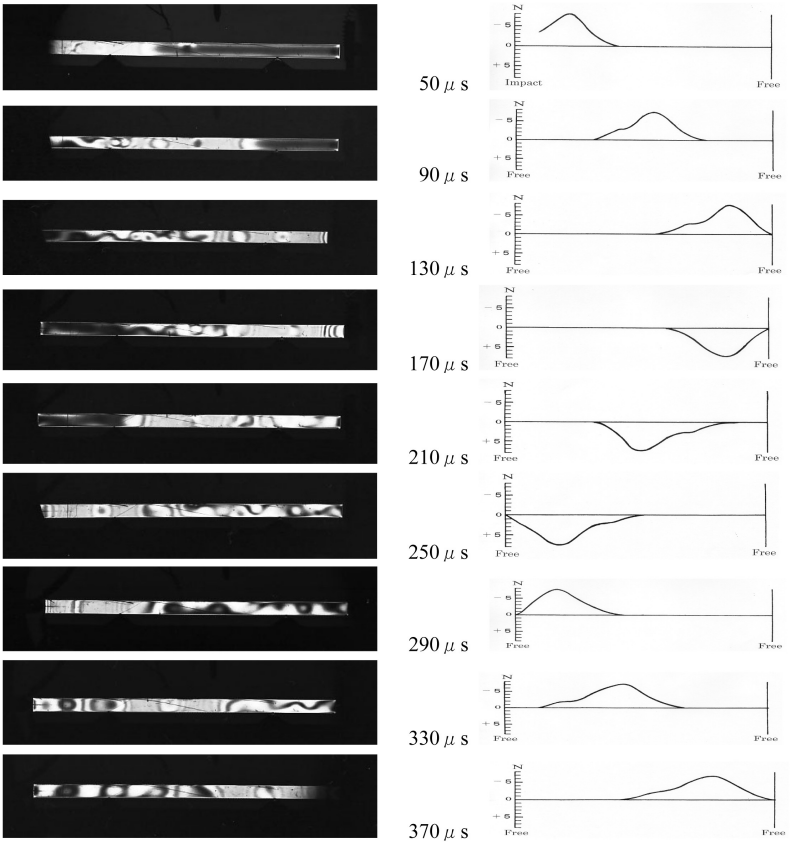

Fig. 3. Dynamic isochromatic fringe patterns and fringe order distributions in rectangular epoxy bar at 60℃. Times given are measured from the instant of direct projectile impact.

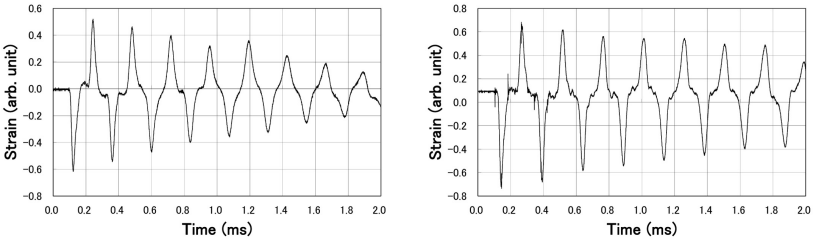

(a) T = 21℃ (b) T = 60℃

Fig. 4. Strain–time relation for rectangular epoxy bar of width 12 mm, thickness 6 mm, and length 201 mm at 21℃ (a) and 60℃ (b) after direct projectile impact.

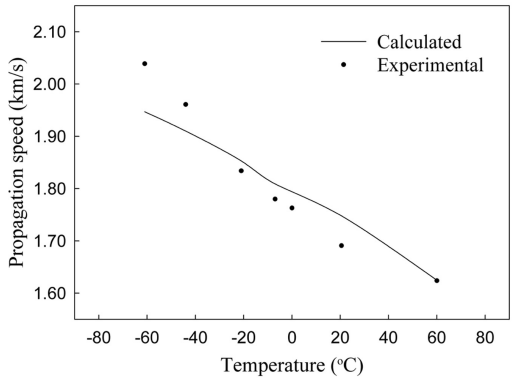

Fig. 5. Propagation speed of stress waves versus temperature for rectangular epoxy bar of width 12 mm, thickness 6 mm, length 201 mm.

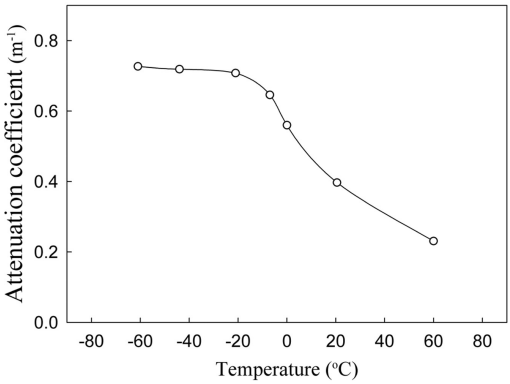

Fig. 6. Attenuation coefficient of stress waves plotted against temperature for rectangular epoxy bar of width 12 mm, thickness 6 mm, length 201 mm.